J Mater Sci: Mater Med (2007) 18:1863–1873
DOI 10.1007/s10856-007-3062-1

Sol-gel-derived TiO_2–SiO_2 implant coatings for direct tissue attachment. Part I: design, preparation and characterization

Virpi Ääritalo · Sami Areva · Mika Jokinen · Mika Lindén · Timo Peltola

Received: 3 May 2005 / Accepted: 12 May 2006 / Published online: 17 May 2007

Abstract A series of sol-gel derived TiO_2–SiO_2 mixed oxide coatings were prepared by carefully controlling the process parameters to obtain silica-releasing coatings consisting of nanoparticles. These features are of paramount importance for enhanced cell adhesion and activation. To achieve both these goals the Ti-alkoxide and Si-alkoxide were first separately hydrolysed and the titania–silica mixed sol was further reacted before the dipping process to obtain the desired particle sizes resulting to the biologically favourable topographical features. Silica release was observed from all the prepared coatings and it was dependent on SiO_2 amount added to the sols, i.e., the higher the added amount the higher the release. In addition, calcium phosphate was able to nucleate on the coatings. From the obtained SiO_2 dissolution data, together with the detailed XPS peak analysis, the mixed oxide coatings are concluded to be chemically heterogeneous, consisting of TiO_2 and SiO_2 species most likely linked together by Ti–O–Si bonds. TiO_2 is chemically stable making long-term implant coating possible and the desired nanoscale dimensions were well preserved although the composition was changed as a consequence of SiO_2 dissolution under in vitro conditions.

V. Ääritalo · M. Jokinen · T. Peltola
Department of Prosthetic Dentistry and Biomaterials Research, Institute of Dentistry, University of Turku, Lemminkäisenkatu 2, 20520 Turku, Finland

S. Areva (✉) · M. Lindén
Department of Physical Chemistry, Åbo Akademi University, Porthansgatan 3-5, 20500 Turku, Finland
e-mail: sami.areva@utu.fi

S. Areva · M. Jokinen · T. Peltola
Turku Centre for Biomaterials, Itäinen Pitkäkatu 4B, 20520 Turku, Finland

Introduction

Due to their ability to form calcium phosphate (CaP) on their surface, sol-gel derived titania (TiO_2) coatings can be considered as an alternative for the more widely used bioactive ceramic-based coatings (hydroxylapatite, bioactive glasses) to ensure implant-bone contact [1]. Although sol-gel derived titania coatings provide interesting features, their potential in biomaterial applications has not been fully exploited. It was recently discovered that, in addition to bone contact, sol-gel derived titania coatings facilitate direct soft tissue attachment (i.e., without fibrous capsule formation), making sol-gel derived titania coatings more widely applicable than coatings having only osteoconductive properties [2]. To date, only certain bioactive glasses have been shown to attach directly to soft tissues without the fibrous capsule formation [3]. In analogy with bioactive glass, the TiO_2 coatings with a good soft tissue attachment are the same that work in bone, but it is not clear whether the same specific properties control both types of tissue response. Although the bioactive glasses directly attached to the soft tissue through the in situ formed CaP layer, a fibrous capsule surrounded the ready made CaP ceramics when implanted in soft tissues [4–7].

According to current paradigm, the bone attachment ability of the sol-gel derived titania coatings and bioactive ceramic coatings results from their ability to form a bone-like calcium phosphate (CaP) on their surface in vitro and in vivo [1, 8–10]. However, it was found that the formation of thick bone-like CaP layer on sol-gel titania coating was not necessary for their direct soft tissue attachment. The titania coating induced the formation of amorphous CaP in situ in the soft tissue environment [2]. The high-reactivity of the sol-gel derived titania coating is based on its tailor-made surface nanostructure, i.e., surface ‘‘pore size’’

distribution (5–50 nm) and chemistry (zeta potential), which were modified by controlling the sol properties and coating parameters. It should be noted that here the ''pore size'' distribution value is estimated from the AFM images of the nanoparticulate coatings as described in [9]. In addition to the well-known effect surface microroughness has on bone response [11–14], the nanometerscale roughness has also been observed to influence osteoblast and osteoclast activation as well as fibroblast and endothelial cell adhesion [15–18]. In particular, it was found that the cell response was enhanced in the presence of ceramic nanoparticles less than 100 nm in diameter [15, 16], which corresponds to the tailor-made surface dimensions of the titania coating, since the coatings are also composed of nanoparticles resulting in the above-mentioned surface nanotopographical features. The enhanced cell response may result from the prerequisite protein adsorption, which is also influenced by the nanodimensions [15]. In addition, bone-forming cells can also be activated by soluble silica, which may explain why some of the silica-releasing materials are osteoinductive [19–22]. The cell activating effect of nanoscale surface roughness and the bone-forming cell activating silica release can be combined in the sol-gel derived TiO_2–SiO_2 mixed oxide films by carefully controlling the process parameters.

Although sol-gel derived titania and silica [1] has been shown to be bioactive, the use of mixed silica–titania films as implant coatings has not been extensively studied [23]. The studied mixed titania–silica oxide coatings were mesoporous in the range of 20–50 nm, but did not show any bioactivity in vitro due to their smoother topography compared to the titania surfaces. In addition, it was not determined whether the studied mixed oxide coating could release silica to activate bone-forming cells. Thus, according to the recent findings related to bone-forming cell activation by released silica and the soft tissue attachment of titania coatings a thorough re-evaluation on the use of titania–silica mixed oxide coatings is needed.

The aim of part I of this paper is to describe in detail the preparation, surface characteristics, bioactivity, protein adsorption and silica release of a series of titania–silica mixed coatings. Results from this study should be correlated with the results in the forthcoming part II of this paper, where the study will be extended to the evaluation of cell responses.

Materials and methods

Pre-treatment of substrates

In this study the titania (TiO_2), silica (SiO_2) and titania–silica (TiO_2–SiO_2) sol-gel derived coatings were prepared on titanium substrates (2×5 cm^2) by the dip-coating method. Titanium substrates were ground by silicon carbide papers having 500, 800 and 1200 grits (R_a values of 0.23, 0.17, 0.15 μm, respectively). The substrates were ultrasonically washed 5 min in acetone and 5 min in ethanol before dipping.

Preparation of sols

The TiO_2 sol was prepared as follows: tetraisopropylorthotitanate [TIPT, $Ti((CH_3)_2CHO)_4$] was dissolved into ethanol and mixed with the solution containing ethyleneglycolmonoethylether ($C_2H_5OCH_2OH$), deionized water, fuming hydrochloric acid (HCl, 37%) and ethanol. The sol was aged 24 h at 0 °C before dipping.

The SiO_2 sol contained tetraethyl orthosilicate (TEOS, $Si(OC_2H_5)_4$), ethanol and nitric acid (HNO_3, 65%) as a catalyst. The sol was aged for 1 h at 0 °C with stirring and additionally 1 h under static conditions before dipping.

The TiO_2–SiO_2 sols were prepared by mixing the following TiO_2 and SiO_2 sols in different volumetric ratios. SiO_2 was prepared by mixing TEOS, ethanol and water at room temperature having the $EtOH:Si(OR)_4$, and $H_2O:Si(OR)_4$ molar ratios of 3.7 and 0.27, respectively. The prepared sol was aged at 40 °C for 60 min. TiO_2 was prepared by mixing TIPT, ethanol, nitric acid, and water at room temperature and aged at 40 °C for 30 min having $EtOH:Ti(OR)_4$, $H_2O:Ti(OR)_4$ and $HNO_3:Ti(OR)_4$ molar ratios of 34, 0.11 and 0.70, respectively. The prepared TiO_2–SiO_2 sols were aged at 40 °C for 24 h and cooled down to 0 °C before dipping process. The compositions and the aging times of the prepared sols are shown in Table 1.

Dipping Process

The titanium substrates were dipped into the sols and withdrawing them at a speed of 0.3 mm/s at ambient atmosphere. After that the substrates were heat-treated at 500 °C for 10 min, cooled and washed ultrasonically 5 min in acetone and 5 min in ethanol and dried in air. This cycle was repeated five times.

In vitro experiments

The bioactivity of the coatings and silica release were studied by immersing the coatings (10×10 mm^2) in 22 mL of simulated body fluid (SBF) [24] at 37 °C for up to 4 weeks. SBF was prepared by dissolving reagent chemicals of NaCl, $NaHCO_3$, KCl, $K_2HPO_4{\cdot}3H_2O$, $MgCl_2{\cdot}6H_2O$, $CaCl_2{\cdot}2H_2O$ and Na_2SO_4 into deionized water. The solution was buffered at physiological pH 7.40 at 37 °C with hydrochloric acid (2 M HCl). The ion concentrations of SBF (Na^+ 142.0, K^+ 5.0, Mg^{2+} 1.5, Ca^{2+} 2.5, Cl^- 147.8,

Table 1 The used parameters for sol preparation

TiO_2:SiO_2 mol-%	EtOH: alkoxide	H_2O: alkoxide	Acid: alkoxide	Oxide content, g /100 mL	Aging
100:0	8.2	1.00	0.018	9.52	24 h at 0 °C
90:10	16.39	1.18	0.30	5.75	24 h at 40 °C
70:30	13.16	1.14	0.23	6.87	24 h at 40 °C
50:50	9.93	1.10	0.17	8.05	24 h at 40 °C
30:70	6.72	1.06	0.10	9.97	24 h at 40 °C
10:90	3.51	1.02	0.03	13.62	24 h at 40 °C
0:100	12.07	14.7	0.60	4.95	1 h at 0 °C

HCO_3^- 4.2, HPO_4^{2-} 1.0, SO_4^{2-} 0.5 mM) are nearly equal to that of human plasma. Three parallel coatings were immersed in closed polyethylene tubes and the tubes were placed in a shaking water bath having a constant temperature at 37 °C. After immersion the coatings were removed from the fluid, gently rinsed with distilled water and dried at 40 °C before surface analysis.

Additional SBF tests complemented with fetal calf serum (1% v/v) were performed to analyse the amount of adsorbed protein on the surface. The samples were immersed for 30 min in serum containing SBF and fixed with descending ethanol series before surface analysis.

Ion concentration analysis

The calcium and silica concentrations in the SBF were monitored as a function of immersion time. Silica concentration was measured using UV–visible spectrophotometer (Shimadzu UV-1601) by the molybdenum blue method. The calcium concentration was measured by microplate photometer (Labsystems, Multiskan EX) using the *o*-cresolphtalein complexone method. Titania concentration in the SBF solutions was measured by UV–visible spectrophotometer using 2% (w/v) hydrogen peroxide and sulphuric acid solution to obtain a titania complex having an adsorption maximum at approx. 380 nm.

Surface analysis

The changes of surface characteristics were determined as a function of immersion time as follows. The morphology and chemical composition of the samples were performed using SEM-EDS [JEOL Scanning Electron Microscope JSM-5500, equipped with an energy dispersive spectroscopy (EDS)]. The elemental analysis was done by carefully adjusting the measurement parameters such as the beam energy, current and angle, spot size, scan size and sample distance so that the signal from the substrate was excluded and only the coatings were analysed, which was achieved when the Ti/Si ratio remained constant directly indicating that only the signal from the coatings were analysed. The XPS [Perkin–Elmer PHI 5400 ESCA System spectrometer] was used to identify the elemental composition of the outermost part of the films. The XPS measurements were performed at a base pressure of 1×10^{-8} Torr using the Mg K_α X-ray (λ = 1253.6 eV) source with the grazing angle of 45°. The UNIFITTU (version 2.1) software was used for peak fitting and quantitative chemical analysis, applying sensitivity factors given by the manufacturer of the instrument. The high-resolution spectra were charge compensated by setting the binding energy (BE) of the C 1s contamination peak to 284.6 eV. The nanoscale surface dimensions of the coatings were characterized by the non-contact tapping mode AFM [NanoScope III multimode AFM; Digital Instruments, Santa Barbara, CA]. The approx. ''pore size'' of the surfaces was determined from the obtained AFM images utilizing a CAD program (Rhinoceros Beta) as previously described by Peltola et al. [9]. Briefly, the distance distributions between the peaks (describing the lateral surface topography and the approx. ''pore size'' distribution) were calculated from the AFM line profiles (describing the vertical surface topography). At least nine line profiles were analysed per sample. A thin-film Philips X-Ray Diffractometer (PW 3710) with Cu K_α radiation was used for the X-ray diffraction (XRD) experiments to determine the crystal structure of the coatings. The diffractometer was operated at 40 kV, 40 mA with a scanning speed of 0.013°/s at 2θ-steps of 0.020°. The angle of incident beam was 2.5° and the 2θ-range of the measurement was 20°–50°. The contact angles of the coatings were measured using the sessile drop method. At least two samples of each film were measured and the contact angles were taken as a mean value from at least 9 individual measurements.

Results

Chemical composition and molecular structure

The bulk compositions of the coatings obtained by EDS analysis confirm that the overall Ti:Si ratios were the same as the Ti:Si ratios of the respective sols (Fig. 1). However, the more surface sensitive XPS analysis of the coatings

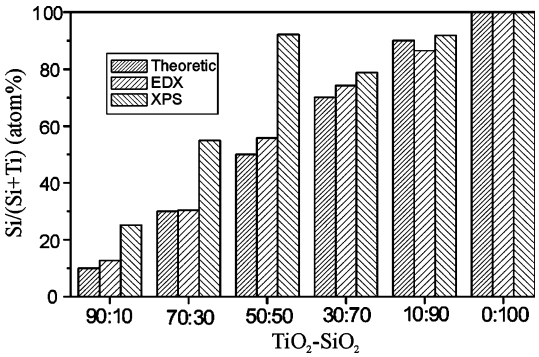

Fig. 1 The amount of Si of the prepared coatings obtained from the EDS and XPS analysis compared to the theoretical values (estimated error 10%)

showed higher than theoretical silica concentrations especially when the theoretical silica content was 50% (i.e., the coating indexed as TiO_2–SiO_2 (50:50)) or lower (Fig. 1). This indicates that the silica is enriched on the outermost surface of these coatings. However, it should be emphasized that the obtained XPS concentrations are accurate only to within about 10%.

The binding energies (BEs) of the Si(2p), Ti($2p_{3/2}$) and O(1s) peaks obtained from the XPS data were more closely analysed to obtain more information on the molecular structure of the coatings. The BE of the Si(2p) peak was at 103.6 eV for the pure SiO_2 coating. The BE shifted towards lower values as the amount of TiO_2 increased in the coating (Table 2). The BE of the Ti(2p3/2) for the pure TiO_2 coatings was at 458.6 eV, which shifted upwards as the SiO_2 content was increased (Table 2). Such an upward shift continues when the SiO_2 content increases from 50% to 90%. Except for the TiO_2–SiO_2 (50:50) coating, where the detected amount of silica on the surface was approx. 90%, the BE changes are in good agreement with the amount of silica calculated from the XPS data (Table 2). In addition, another Ti($2p_{3/2}$) peak appears when the SiO_2 content is more than 30% at lower BE (Table 2) suggesting either changes in Ti coordination number or the presence of two titania species, e.g., Ti–O–Ti and Ti–O–Si. This aspect will be discussed in more detail later. The major O(1s) peak for the pure TiO_2 was at 529.8 eV, which also shifts upwards when the amount of SiO_2 is increased. In addition, two distinct O(1s) peaks appear when the SiO_2 contents was 30% or higher, which can be associated with SiO_2 (higher BE) and TiO_2 (lower BE) (Table 2).

Table 2 Binding energies (eV) of the components calculated from the high-resolution XPS data

TiO_2:SiO_2 mol-%	O (1s)	Ti ($2p_{2/3}$)	Si(2p)
100:0	529.8 (79)	458.6 (100)	
	531.2 (13)		
	532.2 (8)		
90:10	530.0 (70)	458.7 (100)	102.2 (100)
	531.6 (26)		
	532.9 (4)		
70:30	530.4 (43)	459.0 (100)	102.5 (100)
	532.1 (57)		
50:50	531.8 (33)	458.2 (10)	103.1 (100)
	532.7 (67)	459.4 (90)	
30:70	531.1 (29)	457.8 (15)	103.0 (100)
	532.6 (71)	459.4 (85)	
10:90	531.6 (15)	458.3 (15)	103.4 (100)
	532.8 (85)	460.1 (85)	
0:100	533.0 (100)		103.6 (100)

Percentage (%) of the individual component is shown in brackets

Morphology

From the SEM images, it was observed that the coatings are quite smooth and morphologically similar independent of the silica content (Fig. 2). In the AFM images (Fig. 3), the observed micrometer scale morphology results from the grinded titanium substrate and the observed nanometer scale roughness results directly from the nanoparticles or their aggregated structures. In addition, the calculated ''surface pores'' from the AFM images showed that the ''pore size distributions'' were between 2 nm and 50 nm for all coating compositions. However, the SiO_2 surface was clearly composed from smaller particles or aggregates compared to the TiO_2 surface resulting to smoother surface (Fig. 3). The rougher TiO_2 surface is produced by larger particles and/or aggregate structures. Further, the AFM line profiles show that the addition of silica results in smoother surface structure as compared to the TiO_2 coating. The increased silica content in the coating results in fewer aggregated structures or slightly smaller particles and thus smoother surfaces.

Crystal structure

The most intensive reflections in the XRD pattern (Fig. 4) originated from the [100], [002] and [101] reflections of the Ti-metal substrate at approx. 35.1, 38.3 and 40.3° (in 2θ), respectively. In the pure TiO_2 coating the anatase reflections [101] at approx. 25.4° and [200] 48.0° were observed as well as weak rutile reflection [110] at 28°. Anatase reflections were also observed in the TiO_2–SiO_2 (90:10) coatings, but disappeared after the SiO_2 content was further increased indicating that the crystallites are very small or complete loss of crystallinity.

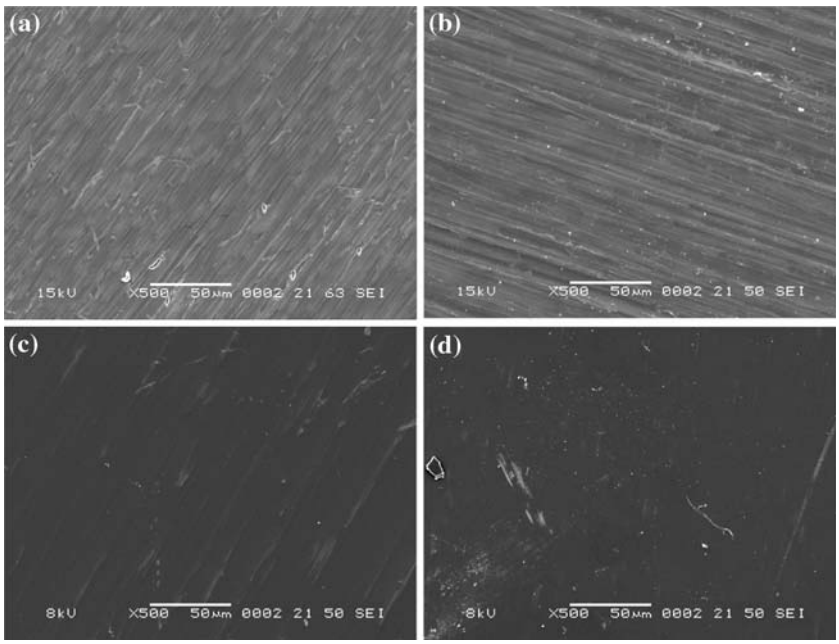

Fig. 2 SEM images of the TiO_2 coating (**a**), and the TiO_2–SiO_2 coatings (70:30) (**b**), (30:70) (**c**), and (10:90) (**d**)

Surface reactivity and dissolution in SBF

The coatings were immersed in SBF to study the CaP formation and silica release during the immersion. The calcium concentration decrease, which is indicative to the CaP formation, was observed only for the pure TiO_2 coatings after day 4 (not shown) in agreement with our previous report [25]. In addition, SEM–EDS revealed no formation of CaP on the mixed TiO_2–SiO_2 coatings. However, the survey XPS spectra showed the presence of both Ca and P after 21 days of immersion for all the SiO_2 containing coatings (Fig. 5). It should be noted that only a trace amount of calcium was observed on the uncoated titanium metal reference. In addition, the Ca and P peaks were observed already after the first sample retrieval point (2 days) in the high-resolution XPS spectra on all the coatings (not shown). The BEs of Ca(2p) and P(2p) were approx. 347.3 eV and 133.2 eV, respectively, corresponding to the CaP phases. Since the BEs of different CaP phases do not differ significantly, the identification of the CaP phase present on the coatings is not possible. However, the Ca/P ratios of the nucleated CaP particles (at day 21) were approx. 1 corresponding to an amorphous CaP phase [25] indicating the absence of partly crystalline bone-like CaP on the surfaces. Thus, all mixed TiO_2–SiO_2 coatings were able to nucleate CaP although their growth was not observed in the solution analysis during the used immersion time.

From the titania solution analysis no evidence was found of soluble titania species even with very high-sample to volume ratios (1 cm^2/4 mL). The silica concentration analysis from the SBF solution showed, however, detectable amounts of released silica from the pure SiO_2 coating and from the TiO_2–SiO_2 (10:90) and (30:70) coatings (Fig. 6). The constant silica level was obtained for the pure SiO_2 already after 2 days. However, the silica dissolution continued from the TiO_2–SiO_2 (10:90) and (30:70) coatings during the whole experiment. The SiO_2 concentration were in ''in sink'' condition (where the SiO_2 amount in solution does not affect the dissolution from the material, which is about 30 ppm for SiO_2) during the whole experiment. In addition, after 28 days of SBF immersion the total amount of Si as measured by EDS showed approx. 90%, 72% and 51% decrease for the pure SiO_2 coating and TiO_2–SiO_2 (10:90) and (30:70) coatings, respectively (Fig. 7). In addition, the amount of Si decreased also in the TiO_2–SiO_2 (50:50) coating, although no silica was observed in the solution analysis (which is probably due to the detection limit of the used solution analysis method). More evidence on the silica release was obtained from the XPS analysis of the coatings measured after the 28 days of SBF immersion (Fig. 8). Significant decrease in the Si amount was observed for all the mixed TiO_2–SiO_2 coatings indicating that SiO_2 is released from the outermost surface from all the coating, although this was not observed in the solution and EDS analysis for the coatings with small SiO_2 content. It should be noted that the substrate originating Ti peaks influences the chemical analysis for the pure SiO_2 coating after the dissolution test. In fact, after dissolution the Ti peak from the substrate was observed even with the surface sensitive XPS method indicating that only a few nanometers thick SiO_2 layer remained. Furthermore, the BEs of the Si(2p) and Ti(2p) peaks were 101.9 and 456.5 eV, respectively, for all the coatings after the silica

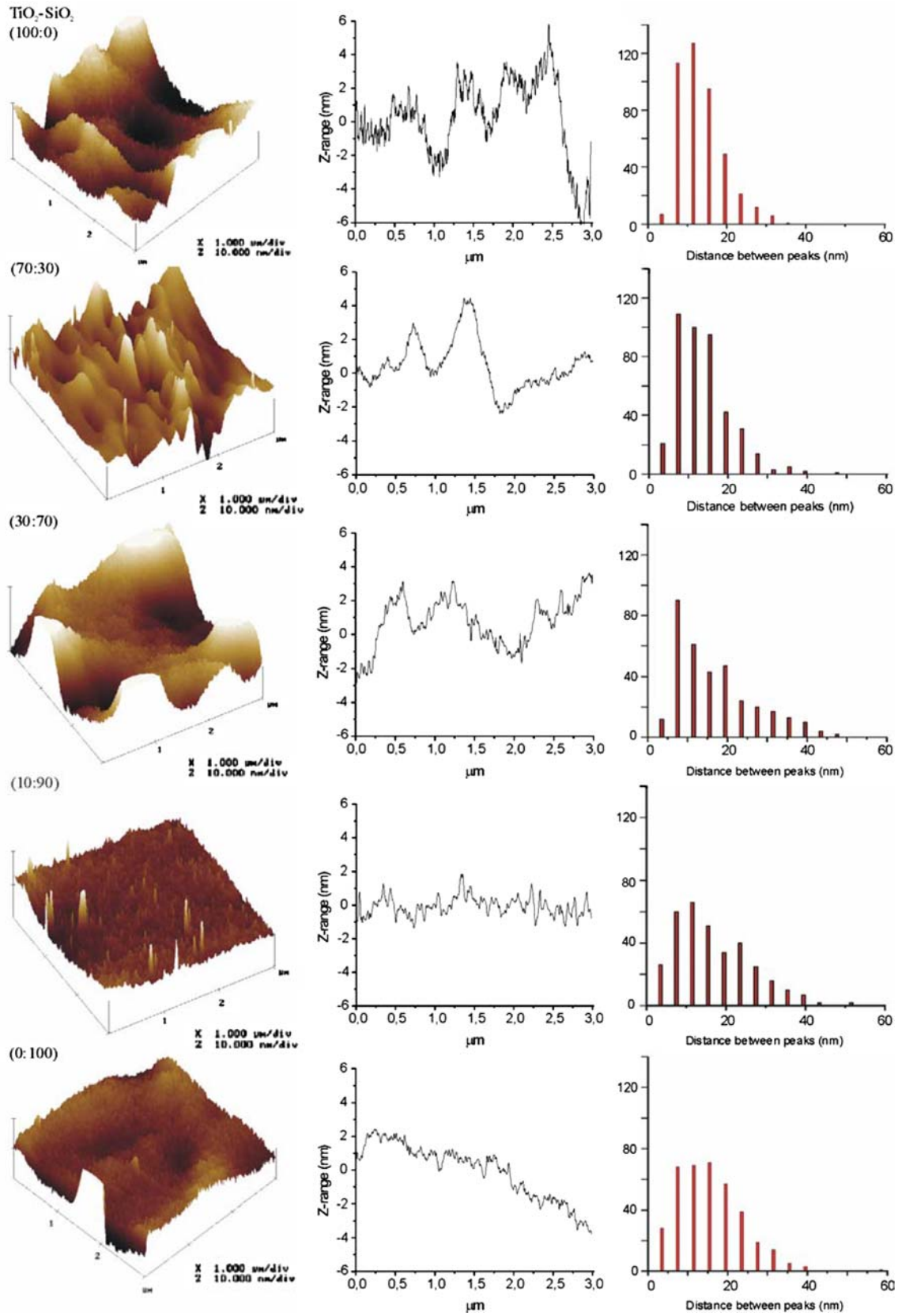

Fig. 3 3D AFM images of the prepared coatings with a representative line section curve and the calculated peak distance distribution histograms showing the average ''pore size'' distribution of the coatings

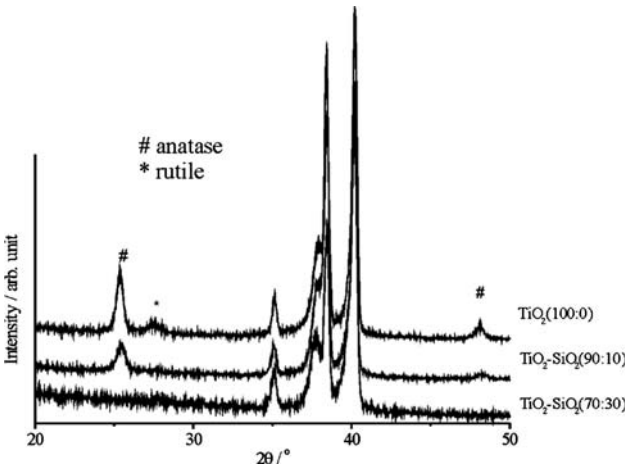

Fig. 4 XRD spectra of the TiO_2 coating and the TiO_2–SiO_2 coatings (90:10) and (70:30)

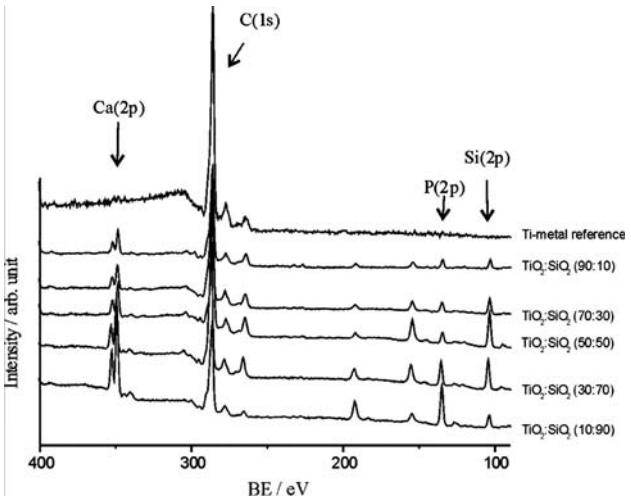

Fig. 5 XPS survey spectra of the coatings after immersion in SBF for 21 days

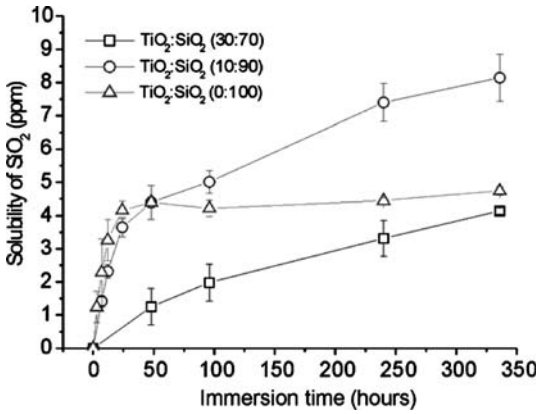

Fig. 6 Evolution of the SiO_2 concentration of the TiO_2–SiO_2 coatings (30:70), (10:90), and (0:100) as a function of SBF immersion time

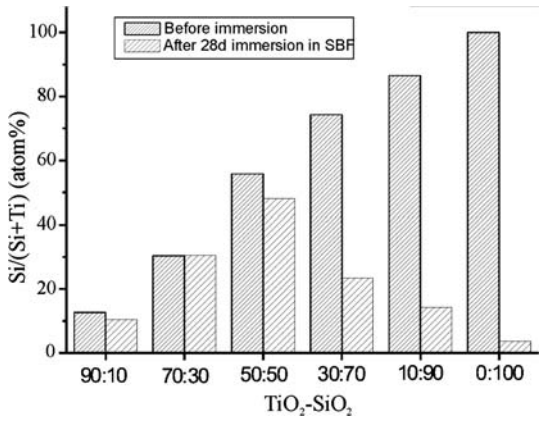

Fig. 7 The amount of Si as obtained from EDS analysis before and after SBF immersion (estimated error 10%)

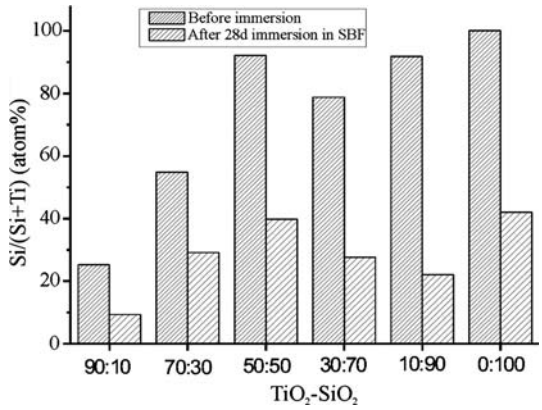

Fig. 8 The amount of Si as obtained from XPS analysis before and after SBF immersion (estimated error 10%)

dissolution. Thus, the upward shift of these peaks observed in the as-prepared coatings was not observed after the silica had been released from the coatings surface.

Because significant Si decrease was observed on the outermost surface after SBF immersion, additional AFM analysis was performed after 7 days of immersion in order to get information on the topographical changes due to silica release. Interestingly, it was noted from the ''pore size analysis'' that the silica dissolution did not affect the coatings ''pore size'' of the mixed oxide coatings compared to pure SiO_2 (Fig. 9). However, the surfaces become rougher (i.e., the vertical topography) due to the SiO_2 dissolution, which can be best observed from the 3D images of coating TiO_2–SiO_2 (30:70) (Fig. 10). This indicates that despite their solubility the surface nanotopography remains in the previously described suitable range for a number of biological applications [15–18].

Additional SBF test were performed including protein to obtain general information on the protein adsorption, since the protein adsorption capability is also important in

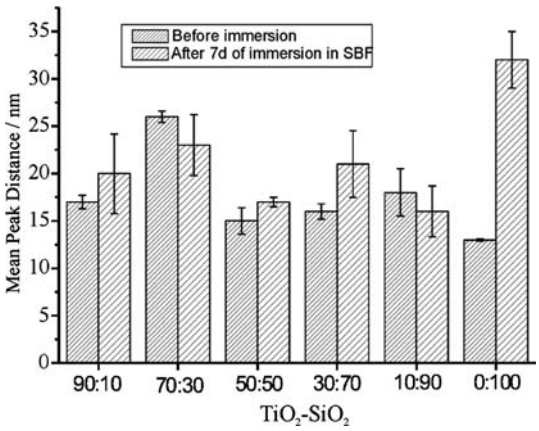

Fig. 9 The average ''pore size'' distributions as obtained from the AFM image analysis of the coating before and after 7 days immersion in SBF

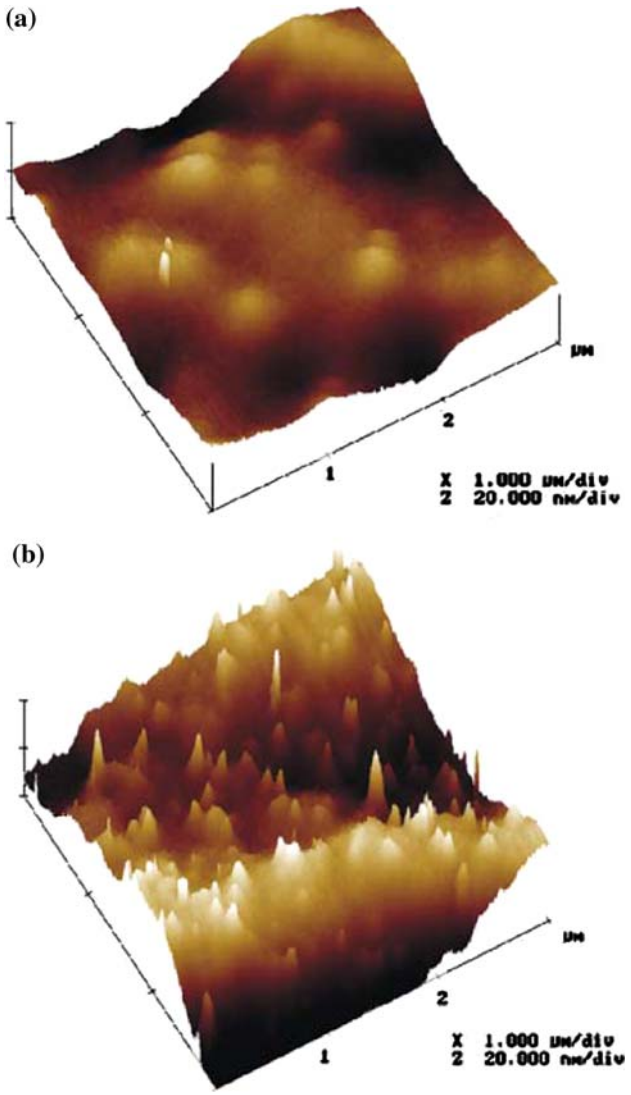

Fig. 10 3D-AFM images of the TiO_2–SiO_2 (30:70) coating before (**a**) and after 7 days (**b**) of immersion in SBF

materials integration to tissues. Because in the XPS analysis no N(1s) peaks were detected for the as-prepared samples, the N/(Ti + Si) ratio is directly related to the amount of adsorbed protein after the immersion in SBF supplemented with proteins. The amount of protein increased as the amount of SiO_2 was increased to 30% compared to pure TiO_2 after which the amount of adsorbed protein decreased when further increasing the SiO_2 content (Fig. 11). In addition, a slight trend was observed in the coatings hydrophobicity/philicity, as measured by the water contact angle, and the amount of adsorbed protein (Fig. 11). The most hydrophobic TiO_2–SiO_2 (70:30) coatings had the highest N/(Ti + Si) ratio.

Discussion

According to the recent findings, for an implant coating to perform well in tissue environment its surface nanostructure, charge and CaP formation ability should be optimised. In bone environment additional advantage can be obtained by releasing silica, which has been shown to activate bone-forming cells resulting in enhanced bone growth [19–21]. To achieve these goals, a series of sol-gel derived mixed TiO_2–SiO_2 coatings were prepared. Such mixed materials have been widely utilized in catalysis and optical applications [26]. In those applications, it is essential that the materials are chemically homogeneous. In contrast to many applications, heterogeneous TiO_2–SiO_2 materials are potential in biological applications, because of the possibility for silica release. However, due to the different hydrolysis and condensation rates of the Ti- and Si-alkoxides special care must be taken in the synthesis step in order to obtain homogeneous or heterogeneous materials.

Theoretically, the addition of Ti-alkoxide to prehydrolysed Si-alkoxide should result in homogeneous materials,

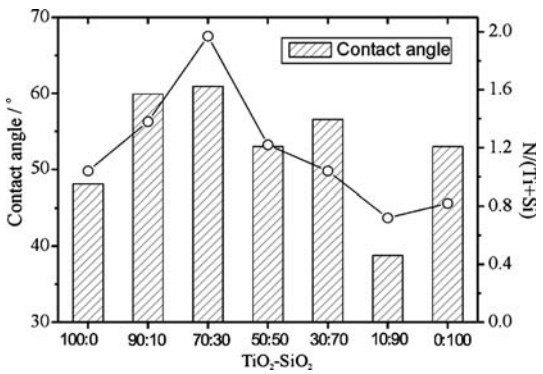

Fig. 11 Water contact angles (error bars ± 5°) of the prepared coatings compared to the amount of adsorbed protein as estimated from the relative amount of surface bound N from the XPS analysis (estimated error 10%)

since homocondensation of the silicates is slow with respect to the heterocondensation reaction [27]. However, with this method homogeneous TiO_2–SiO_2 oxides can only be obtained at low TiO_2 content, with the maximum TiO_2 concentration less than 15 wt%. In higher concentrations some of the Ti atoms do not react with the silica and TiO_2 tends to form as a separate phase [23]. The best homogeneity over the whole TiO_2–SiO_2 concentrations range has been obtained by two-stage hydrolysis procedure, where the addition of Ti-alkoxide to prehydrolysed Si-alkoxide was followed by the addition of water and acid to complete the reaction [28]. Thus, the chemical homogeneity of the mixed oxide materials is highly dependent on the used preparation method. The chemical homogeneity is usually associated with the relative amount of Ti–O–Si bonds and has been quantified, for example, using XPS and IR methods [23, 29–31].

In this study, the aim was to obtain silica-releasing coatings consisting of particles having the suitable size range for biological applications. To achieve both these goals, the Ti-alkoxide was first thoroughly reacted before the addition of mildly hydrolysed Si-alkoxide. The titania–silica mixed sol was further reacted before the dipping process to obtain the desired particle sizes resulting to the biologically favourable topographical features. In contrast to the above-mentioned preparation methods, the objective of this procedure was to obtain a heterogeneous sol, where the colloidal titania particles could crystallize into TiO_2 surrounded by an amorphous SiO_2 connected by Ti–O–Si bonds during drying and calcination.

The outermost surface of the obtained morphologically smooth TiO_2–SiO_2 surfaces (Fig. 2) were slightly enriched by Si (Fig. 1) and consisted from ''pore sizes'' of approx. 2–50 nm (Fig. 3), which has been previously shown beneficial for the CaP nucleation [9]. When the amount of SiO_2 was lower than 70%, the SiO_2 surface enrichment became more pronounced. In general, the surfaces became smoother as the amount of SiO_2 increased. Although the SBF solution analysis showed no CaP formation on the TiO_2–SiO_2 coatings, XPS analysis showed that all coatings were able to nucleate CaP in SBF (Table 2 and Fig. 5). Similarly, the solution analysis showed silica release only from coatings containing 70% or more SiO_2 (Fig. 6) while the EDS and XPS analysis suggested that some (but not all) of the SiO_2 had dissolved from all the coatings (Figs. 7 and 8). Thus, silica was released from all the coatings from both the bulk and surface structures, although the topography was only slightly influenced (Fig. 9). Thus, except for the silica release, the morphology of the coatings do not dramatically change during the early stages of immersion (day 7), which can be related to the insolubility of the titania particles of the films. In addition to the CaP formation ability, it is well known that protein adsorption also influences the materials biological behaviour [32]. It was found that the contact angles indicating hydrophobicity/philicity, which were not dependent on the amount of silica, correlated with the amount of absorbed protein on the surface (Fig. 11). Although there are a number of surface properties that influence protein adsorption, such as electrical charge, the adsorption data of this study is in line with the general findings that the more hydrophobic the surface the greater the extent of protein adsorption [33]. These results further suggest that the TiO_2–SiO_2 (70:30) coating, which adsorbed the highest amount of protein on its surface, would be the most potential in applications where the amount of released silica is not crucial, e.g., in soft tissues.

The XPS results showed an upward shift in the Ti($2p_{3/2}$) BE from 458.6 to 460.1 eV as the amount of SiO_2 increases (Table 2). Such an upward shift has been usually explained by the decrease of Ti coordination number, resulting from the increasing interatomic potentials due to decreasing bond length, suggesting that Ti ions obtain the tetrahedral coordination of the SiO_2 matrix at high-SiO_2 concentrations [23]. Thus, the observed changes in BE values of Ti, Si and O can be associated with the formation of Ti–O–Si bonds. However, the two O(1s) peaks could be associated to TiO_2 and SiO_2 species (Table 2) and no distinct O(1s) peak resulting from Ti–O–Si bond was observed. From these findings, it can be speculated that thoroughly homogeneous coatings were not obtained but rather the TiO_2–SiO_2 interface consist of isolated TiO_2 particles surrounded by an amorphous SiO_2 possibly cross-linked by Ti–O–Si bonds in a continuous structure, although the extended 3D network of Ti–O–Si is not present. This is in agreement with an earlier report by Lassaletta et al. [34] suggesting that, in addition to the effect of coordination environment, also the TiO_2–SiO_2 interface influences the BEs due to changes in photoelectron screening properties. In addition, Goncalves et al. [35] also argued based on X-ray adsorption measurements that also octahedrally coordinated Ti atoms show upward shifting in their BEs. Although crystalline anatase TiO_2 was observed only in TiO_2–SiO_2 (90:10) coating (Fig. 4), the presence of isolated TiO_2 particles, albeit amorphous, also at high-SiO_2 contents is supported by the two distinct Ti($2p_{3/2}$) peaks (Table 2). In addition, the relative amount of the O(1s) peaks assigned to Ti–O–Ti compared to Si–O–Si increases as the amount TiO_2 increases in the coatings. Additional proof for the heterogeneous structure of the coatings is the fact that these coating are able to release silica in contrast to the homogeneous TiO_2–SiO_2 materials. This can be rationalized by the fact that the silica dissolves readily from separate SiO_2 particles. It should be noted, however, that the BEs are also influenced by the presence of other moieties and the possibility of differential charging making the interpretations with literature values ambiguous [36].

Since the released SiO_2 concentration were well below the limit for the ''in sink'' conditions during the whole release experiments, the observed levelling of the SiO_2 concentration after the initial burst for the pure SiO_2 coating results from the fact that almost all of the SiO_2 is quickly dissolved from the coating (Fig. 6). The EDS and XPS analysis where the Ti substrate peaks appeared after the dissolution experiment also supports this conclusion (Figs. 7, 8). The dissolution rate from the TiO_2–SiO_2 coatings (10:90) and (30:70) is constant, after the initial burst, during the whole experiment. The degradation of bioresorbable sol-gel derived SiO_2 matrixes is usually a combination of bulk degradation and surface erosion, which are dependent on both the chemical and pore structures of the matrixes [37, 38]. The release rates, calculated from the linear part of the release curve, were 0.0132 and 0.0093 ppm/h for the TiO_2–SiO_2 coatings (10:90) and (30:70), respectively. When these release rates are normalized by the SiO_2 content it can be concluded that the SiO_2 release is mostly influenced by the SiO_2 amount present in the coatings, although their surface porosity and chemical structure were slightly different. The observed initial burst and the XPS analysis showing decreased amounts of silica on their outermost surfaces also indicates that the oxides are heterogeneously mixed in the coatings. Furthermore, SiO_2 did not dissolve completely from the coatings indicating that the TiO_2 and SiO_2 species are linked together by Ti–O–Si bonds and not appearing as separate particles.

Bioglass® 45S5 (which contains 45% SiO_2) forms rapidly a CaP layer on its surface due to the surface reaction associated with SiO_2 dissolution that was recently found to stimulate osteogenesis in vitro [19]. It was then shown that the dissolved ionic products regulated the gene-expression of the bone-forming cells [20]. It was further shown that during the critical steps in cell cycles the amount of released SiO_2 in solution was from approx. 20 to 40 ppm [21]. However, a systematic gene-expression study of the bone-forming cells with varying SiO_2 concentrations is still lacking and the appropriate SiO_2 levels still remains to be discovered. The levels of dissolved SiO_2 from TiO_2–SiO_2 coatings were somewhat lower than from the Bioglass® 45S5, furthermore, it should be also noted that the amount of released silica depends on the used mass volume ratio. It can be still expected that locally, i.e., in the vicinity of the coatings, the SiO_2 concentrations might reach to a level able to stimulate osteogenesis. In addition, the prepared TiO_2–SiO_2 coatings exhibited the desired nanotopography. Thus, good cell response can be expected to these coatings. Naturally, changing the number of coating layers and heat-treatment conditions could be further used to control the silica-releasing properties. Such studies are currently underway in our laboratory.

Discussion

The silica-releasing sol-gel derived TiO_2–SiO_2 mixed oxide coatings were prepared by two-step hydrolysis of the Ti-alkoxide and Si-alkoxide solutions resulting in heterogeneously mixed oxide phases. TiO_2 is stable making long-term implant coating possible and the desired nanoscale dimensions are well preserved although the composition is changed. In the accompanying part II of this paper the evaluation of these coatings as implant coatings will be extended to cell response studies.

Acknowledgements Dr J. Wolke from the University Medical Centre Nijmegen, Nijmegen, The Netherlands, is acknowledged for his assistance in the TF-XRD measurements. SA would like to thank the Graduate School of Materials Science, Turku, Finland, for financial support. This study was supported by the National Technology Agency, Finland (grant 40725/01).

References

1. P. LI, *In vivo and in vitro calcium phosphate induction on gel glasses*. Ph.D. thesis, University of Leiden, Leiden, The Netherlands (1993)
2. S. AREVA, H. PALDAN, T. PELTOLA, T. NÄRHI, M. JOKINEN and M. LINDÈN, *J. Biomed. Mater. Res.* **70** (2004) 169
3. J. WILSON, G. H. PIGOTT, F. J. SCHOEN and L. L. HENCH, *J. Biomed. Mater. Res.* **15** (1981) 805
4. D.-J. LI, K. OHSAKI II, P.-C. CUI, Q. YE, K. BABA, Q.-C. WANG, S. TENSHIN and T. TAKANO-YAMAMOTO, *J. Biomed. Mater. Res.* **45** (1999) 322
5. H. YUAN, J. D. DE BRUIJN, Y. LI, J. FENG, Z. YANG, K. DE GROOT and X. ZHANG, *J. Mater. Sci: Mater. Med.* **12** (2001) 7
6. H. YUAN, M. VAN DER DOEL, S. LI, C. A. VAN BLITTERSWIJK, K. DE GROOT and J. D. DE BRUIJN, *J. Mater. Sci: Mater. Med.* **13** (2002) 1271
7. E. M. OOMS, E. A. EGGLEZOS, J. G. C. WOLKE and J. A. JANSEN, *Biomaterials* **24** (2003) 749
8. P. LI, I. KANGASNIEMI, K. DE GROOT and T. KOKUBO, *J. Am. Ceram. Soc.* **77** (1994) 1307
9. T. PELTOLA, M. JOKINEN, H. RAHIALA, M. PÄTSI, J. HEIKKILÄ, I. KANGASNIEMI and A. YLI-URPO, *J. Biomed. Mater. Res.* **51** (2000) 200
10. T. PELTOLA, H. PALDAN, N. MORITZ, S. AREVA, J. KORVENTAUSTA, M. JOKINEN, T. NÄRHI, R.-P. HAPPONEN and A. YLI-URPO, *Key Eng. Mat.* **218–220** (2002) 207
11. D. BUSER, R. K. SCHENK, S. STEINEMANN, J. P. FIORELLINI, C. H. FOX and H. STICH, *J. Biomed. Mater. Res.* **25** (1991) 889
12. M. WONG, J. EULENBERGER, R. SCHENK and E. HUNZIKER, *J. Biomed. Mater. Res.* **29** (1995) 1567
13. A. WENNERBERG, T. ALBREKTSSON, B. ANDERSSON and J. J. KROL, *Clin. Oral Impl. Res.* **6** (1995) 24
14. T. HAYAKAWA, M. YOSHINARI, H. KIBA, H. YAMAMOTO, K. NEMOTO and J. A. JANSEN, *Biomaterials* **23** (2002) 1025
15. T. J WEBSTER, C. ERGUN, R. H. DOREMUS, R. W. SIEGEL and R. BIZIOS, *J. Biomed. Mater. Res.* **51** (2000) 475
16. T. J. WEBSTER, C. ERGUN, R. H. DOREMUS, R. W. SIEGEL and R. BIZIOS, *Biomaterials* **22** (2001) 1327

17. M. J. DALBY, M. O. RICHLE, H. JOHNSTONE, S. AFFROSSMAN and A. S. G. CURTIS, *Biomaterials* **23** (2002) 2945
18. M. J. DALBY, M. O. RICHLE, D. S. SUTHERLAND, H. AGHELI and A. S. G. CURTIS, *J. Biomed. Mater. Res.* **69** (2004) 314
19. I. D. XYNOS, M. V. J. HUKKANEN, J. J. BATTEN, L. D. BUTTERY, L. L. HENCH and J. M. POLAK, *Calcif. Tissue Int.* **67** (2000) 321
20. I. XYNOS, A. EDGAR, L. BUTTERY, L. HENCH and J. POLAK, *J. Biomed. Mater. Res.* **55** (2001) 151
21. L. L. HENCH, *Key Eng. Mater.* **192–195** (2000) 575
22. T. YAMAGUCHI, N. CHATTOPADHYAY, O. KIFOR, R. R. BUTTERS, T. SUGIMOTO JR and E. M. BROWN, *J. Bone Miner. Res.* **13** (1998) 1530
23. M. JOKINEN, M. PÄTSI, H. RAHIALA, T. PELTOLA, M. RITALA and J. B. ROSENHOLM, *J. Biomed. Mater. Res.* **4** (1998) 295
24. T. KOKUBO, H. KUSHITANI, S. SAKKA, T. KITSUGI and T. YAMAMURO, *J. Biomed. Mater. Res.* **28** (1990) 721
25. S. AREVA, T. PELTOLA, E. SÄILYNOJA, K. LAAJALEHTO, M. LINDÉN and J. B. ROSENHOLM, *Chem. Mater.* **14** (2002) 1614
26. X. GAO and I. E. WACHS, *Catal. Today* **51** (1999) 233, and the references therein
27. C. J. BRINGER and G. W. SCHERER, *Sol-Gel Science: The Physics and Chemistry of Sol-Gel Processing*, Akademic Press Inc., San Diego, USA (1990) pp 226–227, and the references therein
28. J. B. MILLER, S. T. JOHNSTON and E. I KO, *J. Catal.* **150** (1994) 311
29. S. M. MUKHOPADHYAY and S. H. GAROFALINI, *J. Non-Cryst. Solids* **126** (1990) 202
30. M. AIZAWA, Y. NOSAKA and N. FUJII, *J. Non-Cryst. Solids* **128** (1991) 77
31. M. SCHRAML-MARTH, K. L. WALTHER, A. WOKAUN, B. E. HANDY and A. BAIKER, *J. Non-Cryst. Solids* **143** (1992) 93
32. S. M. SLACK and T. A. HORBETT, *J. Colloid Interface Sci.* **124** (1988) 535
33. T. A. HORBETT and J. L. BRASH (Ed), ''Proteins at Interfaces II: Fundamentals and Applications'', *ACS Symposium Series 602*, Washington D.C., USA (1995)
34. G. LASSALETTA, A. FERNANDEZ, J. P. ESPINOS and A. R. GONZALES-ELIPE, *J. Phys. Chem.* **99** (1995) 1484
35. J. E. GONCALVES, S. C. CASTRO, A. Y. RAMOS, M. C. M. ALVES and Y. GUSHIKEM, *J. Electron Spec. Rel. Phen.* **114–116** (2001) 307
36. F. GARBASSI and L. BALDUCCI, *Microporous Mesoporous Mat.* **47** (2001) 51
37. R. VIITALA, M. JOKINEN, S. TUUSA, J. B. ROSENHOLM and H. JALONEN, *J. Sol-Sel Sci. Tech* **36** (2005) 147
38. R. VIITALA, M. JOKINEN, S. L. MAUNU, H. JALONEN and J. B. ROSENHOLM, *J. Non-Cryst Solids* **351** (2005) 3225